Proceedings of the Korean Nuclear Society Spring Meeting
Pohang, Korea May, 1999

A Phenomenological Liquid Film Dryout Model in Vertical Annulus at High Vapor Quality

S. D. Hong, S. Y. Chun, S. K. Yang, M. K. Chung, C. Park

Korea Atomic Energy Research Institute
Thermal-Hydraulic Experiment Dept.
P.O. Box 105, Yusong,
Taejon, 305-600, Korea

Abstract

A Phenomenological liquid film dryout model for annulus geometry is suggested to calculate critical heat flux at high vapor quality. The initial conditions obtained by the bundle-based flow pattern transition criterion. The constitutive relations of the tube-based entrainment and deposition models are modified by droplet contact area fractions that counting the cold wall effect. The concept of the droplet contact area fraction gives simple modeling of the deposition and entrainment rates on the liquid films of the inner and outer tubes and counts for the observed annulus characteristic that the outer film thickness is thicker than the inner liquid film. The model predicts well at low flow-rate but tends to over-estimate at high flow-rate and shows good results for the broad critical heat flux experimental data(595 data) with the accuracy of the mean of 0.99 and the RMS error of 0.115.

1. Introduction

It is generally recognized that the Critical Heat Flux (CHF) governing mechanism of high quality differs substantially from that of low quality and subcooled CHF. CHF at high quality is often called dryout as the CHF condition occurred when the flow-rate of the liquid film on the heated surface fell to zero; hence the name *dryout*. Whally[1] originally proposed phenomenological Liquid Film Dryout (LFD) model for tube geometry in 1978. It is modified and extended the constitutive relations of entrainment and deposition process on the liquid film surface by several authors (Saito et al.[2]; Levy et al.[3]; Katto[4]; Sugawara[5]; Hoyer[6]). These studies describe that near the CHF condition, the heated surface is covered by liquid film. The heat flow through the liquid film induces evaporation at the surface of the liquid layer and the thickness decreases as the heat flux increases. When the heat flux is high enough to dryout this liquid film, it causes an abrupt rise in the heated surface temperature leading to fuel failure.

Dryout characteristics in annulus are similar to the bundle's because the annulus has the cold wall or large interfacial area. The deposition and entrainment rates of the inner heated tube are relatively lower than the outer tube, and the outer film thickness is thicker than the inner liquid film in annulus. It gives the large discrepancies of CHF values on pressure between tubes and annuli, especially at a low flow rate and high quality. Both quantitative and qualitative study of dryout behavior in tubes and annuli have been done by several investigators (Macbeth[7]; Saito[2]; Doerffer et al.[8]; Park et al.[9]). Macbeth[7] claims that the annulus test section belongs to the family of rod bundles, i.e. 'one-rod bundle'. Doerffer et al. studied the parametric trends of CHF between tubes and annuli quantitatively and pointed out that the CHF decreases in both flow geometries with increasing pressure, especially at low mass flux and high quality, where the deposition-controlled CHF can occur. This is due to the decrease of the deposition coefficient with increasing pressure. This decreasing trend of

the deposition coefficient was observed in tubes and annuli, and it was reported by Saito et al.[2]. The difference in the rate of CHF decreases between these geometries may be associated with the difference in the droplet deposition flow rate on the heated surface. In tubes all deposited droplets reach the heated surface, while in internally heated annuli only a small portion of them deposit on the heated rod. This may be explained by the visual observation of Park et al.[9], in that, the outer liquid film (cold wall side) was generally thicker than the inner film in his CHF experiment. Therefore, if the deposition flow rate becomes lower, the CHF in tubes decreases at a much higher rate than in annuli.

The tube-based LFD model, which uses the heated equivalent diameter of annulus instead of the tube diameter as suggested by Katto(1979)[10] in his generalized correlations, predicts well at high flow rate condition. However the model does not predict correctly at low flow rate (below 600 kg/m^2-s). It is so natural that the previous LFD model is distorted at low flow and high quality conditions by the improper application of the boundary conditions at the onset of annular flow and of constitutive relations for the entrainment and deposition models[18]. In this study, the LFD model presented for the CHF predictions of annuli with some modifications in the initial conditions and the constitutive relations. The flow pattern transition model based on bundle is adopted to define the onset of annular flow location. Liquid film thickness is redefined by considering the cold wall. The constitutive relations for the tube-based entrainment and deposition models are modified by droplet contact area fractions.

2. Modeling

2.1 Governing Equations

Figure 1 shows both the side and cross-sectional view of annular flow pattern in annulus channel. The entrainment, deposition, and evaporating process on the liquid film surface is represented in Figure 2. The governing equation in the liquid film flow set from the location z = z_{an} which is onset of annular flow location (Figure 2). The mass balance equation in the control volume for inner liquid film is

$$\frac{dG_{fi}}{dz} = \frac{4}{d_{he}}\left(D_i - E_i - \frac{q''}{h_{fg}} \right), \tag{1}$$

and outer liquid film is

$$\frac{dG_{fo}}{dz} = \frac{4}{d_{he}}\left(D_o - E_o \right), \tag{2}$$

where q'' is the heat flux, h_{fg} the latent heat of vaporization, d_{he} the heated equivalent diameter, G_{fi}, G_{fo} are flow rates of the inner and outer liquid films, D_i, D_o the droplet deposition rates onto the inner and outer liquid films, E_i, E_o the droplet entrainment rate from the inner and outer liquid film to the vapor core, respectively. Major assumptions of the present LFD model are as follows;

1) Deposition and entrainment rates on the inner or outer liquid films are proportional to the wetted area fraction of the inner or outer tube.
2) The initial film thickness of inner tube has the following relationship with the initial film thickness of outer tube,

$$\frac{\boldsymbol{d}_{ii}}{d_i} = \frac{\boldsymbol{d}_{oi}}{d_o}, \tag{3}$$

where $\boldsymbol{d}_{ii}, \boldsymbol{d}_{oi}$ are the initial thicknesses of inner and outer liquid films, d_i, d_o the inner and outer diameters, respectively.

3) Entrainment rate becomes zero if the liquid film thickness is less than the critical film

thickness, δ_c, given by Katto [4] as

$$\delta_c = 0.00536\,\sigma\rho_g\left(\frac{\rho_g}{\rho_f}\right)^{0.4}\left(\frac{h_{fg}}{q''}\right)^2\left(1+\frac{\rho_g}{\rho_f}\right), \tag{4}$$

where σ is the surface tension and ρ_f, ρ_g are the density of liquid and vapor, respectively.

2.2 Constitutive Relations

If we assumed all film velocities are equal, the total liquid film flow rate can be represented by the inner and outer liquid films as

$$G_f = G_{fi} + G_{fo}\,, \tag{5}$$

The deposition rate to the inner liquid film is

$$D_i = kC\Lambda_i\,, \tag{6}$$

and to the outer liquid film

$$D_o = kC\Lambda_o\,, \tag{7}$$

where k is the specified mass transfer coefficient, C the liquid concentration away from the liquid film and Λ_i, Λ_o are the droplet contact area fractions of the inner and outer tubes as defined below;

$$\Lambda_i = \left(\frac{d_i}{d_o + d_i}\right), \text{ and } \quad \Lambda_o = \left(\frac{d_o}{d_o + d_i}\right).$$

The liquid concentration is written as

$$C = \frac{(G(1-x) - G_{fi} - G_{fo})}{\left\{\dfrac{G\,x}{\rho_g} + \dfrac{G(1-x) - G_{fi} - G_{fo}}{\rho_f}\right\}}. \tag{8}$$

Katto[4] suggested a simplified form for mass transfer coefficient of Whalley [1] as

$$\left.\begin{aligned} k &= 0.405\sigma^{0.915} \qquad for\ \ \sigma < 0.0383, \\ k &= 9.48\times10^4\,\sigma^{4.70} \qquad for\ \ \sigma > 0.0383. \end{aligned}\right\} \tag{9}$$

The entrainment rate from the inner liquid film is given by

$$E_i = kC_{eq}\Lambda_i\,, \tag{10}$$

and fromthe outer liquid film

$$E_o = kC_{eq}\Lambda_o\,, \tag{11}$$

where C_{eq}, an equilibrium concentration, would be in equilibrium with the film flow rate under adiabatic conditions.

The equilibrium concentration can be expressed in terms of hydrodynamic equilibrium quality such that

$$C_{eq} = \frac{(G(1-x_{eq}) - G_{fi} - G_{fo})}{\left\{\dfrac{G\,x_{eq}}{\rho_g} + \dfrac{G(1-x_{eq}) - G_{fi} - G_{fo}}{\rho_f}\right\}}. \tag{12}$$

The hydrodynamic equilibrium quality x_{eq} in the above equation could be obtained by the Levy model[3] as below;.

$$\left.\begin{aligned} x_{eq} &= 1-\frac{G_l/G}{1-\sqrt{1/y}} \qquad for\ Y_f^+ \geq 30, \\ x_{eq} &= 1-\frac{G_l/G}{1-\sqrt{1/y'}} \qquad for\ Y_f^+ < 30, \end{aligned}\right\} \tag{13}$$

where the entrainment parameter y is the root of

$$y = 1+\left[\frac{2}{0.4x_{eq}^2}\frac{s r_f}{G^2 d_{he}}\left\{\left(\frac{r_f}{r_g}\right)^{1/y}-1\right\}\right]^{0.5},$$

and y' is given by

$$y' = 1+\sqrt{2}(y-1).$$

The dimensionless film thickness, Y_f^+, has a triangular relationship with the average film flow rate G_f and wall shear stress t_w as

$$\frac{G_f/r_f}{\sqrt{t_w/r_f}} = \frac{2}{R^+}K(Y_f^+, R^+), \tag{14}$$

where

$$\begin{aligned} K(Y_f^+, R^+) &= \tfrac{1}{2}R^+Y_f^{+2} - \tfrac{1}{3}Y_f^{+3}, && for\ Y_f^+ < 5, \\ K(Y_f^+, R^+) &= 12.51R^+ - 10.45 - 8.05R^+Y_f^+ \\ &\quad + 2.775Y_f^{+2} + 5R^+Y_f^+ \ln Y_f^+ - 2.5Y_f^+ \ln Y_f^+, && for\ 5 < Y_f^+ < 30, \\ K(Y_f^+, R^+) &= 3R^+Y_f^+ - 63.9R^+ - 2.125Y_f^{+2} - 1.25Y_f^{+2}\ln Y_f^+ \\ &\quad + 2.5R^+Y_f^+ \ln Y_f^+ + 573.21, && for\ Y_f^+ > 30, \end{aligned}$$

with

$$R^+ = \frac{R r_f\sqrt{t_w/r_f}}{m_f}, \quad Y^+ = \frac{Y_f r_f\sqrt{t_w/r_f}}{m_f},$$

where R is the heated equivalent radius of annuli and Y_f the distance perpendicular to the wall. If we assume the second order terms of liquid film thickness are negligible, we will have the reduced form for distance, Y_f, as

$$Y_f \approx d_{he}\left(\frac{d_i d_i + d_o d_o}{d_o^2 - d_i^2}\right), \tag{15}$$

where d_i, d_o are the thicknesses of inner and outer liquid films, respectively.

The foregoing shear stress is calculated as

$$t_w = \frac{1}{2}C_{fi}\, r_g\left(\frac{Gx_{eq}}{r_g}\right)^2, \tag{16}$$

where C_{fi} is the interfacial friction factor. Hewitt-Whalley [11] proposed this friction factor as

$$C_{fi} = C_{fg}\left[1+24\left(\frac{r_f}{r_g}\right)^{1/3}\frac{Y_f}{d}\right],$$

and C_{fg} is the vapor single-phase friction factor in a smooth tube, which is given by

$$C_{fg} = 0.079\,\mathrm{Re}_g^{-\frac{1}{4}}.$$

2.3 Onset of Annular Flow and Initial Conditions

On the basis of the Macbeth's[7] study that dryout characteristics in annulus are similar to the bundle characteristics, Venkateswararo's [13] churn-to-annular flow transition model is adopted to define the onset of annular flow location as

$$j_g = 3.1\left[\frac{\sigma g(\rho_f - \rho_g)}{\rho_g^{\,2}}\right]^{1/4} \tag{17}$$

This equation based on the entrainment model is interpreted that churn-to-annular flow transition occurs at the minimum vapor velocity necessary to transport the largest entrained drop in the upward direction. The vapor superficial velocity in the above equation depends only on the fluid property, and the constant 3.1 is less than the Kutateladze number 3.2 which is the flow reversal criterion in a vertical tube suggested by Pushkina-Sorokin [13].

Quality, location and void fraction at the onset of annular flow are

$$x_{an} = \frac{j_g \rho_g}{G}\ , \tag{18}$$

$$z_{an} = \frac{d_{he} G}{4q''}\left(h_f - h_{in} + h_{fg} x_{an}\right), \tag{19}$$

$$\alpha_{an} = \frac{x_{an}}{C_o[x_{an} + \frac{\rho_g}{\rho_f}(1 - x_{an})] + \rho_g \frac{V_{gj}}{G}}, \tag{20}$$

where h_f, h_{in} in equation (19) are enthalpies at saturation and inlet, respectively. The drift velocity and coefficient, V_{gj}, C_o, in equation (20) are chosen as a flow pattern independent model proposed by Dix [14] as

$$V_{gj} = 2.9\left[\frac{\sigma g(\rho_f - \rho_g)}{\rho_f^{\,2}}\right]^{1/4},$$

$$C_o = \beta[1 + (\frac{1}{\beta} - 1)]\ ,$$

where β is the kinematic void fraction.

The initial film thicknesses of inner and outer tubes at the onset of annular flow are assumed as relationship of equation (3). If we neglet second order term ($\delta_{oi}^2 \approx 0$), then the initial outer film thickness could be obtained as

$$\delta_{oi} \approx \frac{(d_o^2 - d_i^2)(1 - \alpha_{an})}{2d_o\left(1 + \left(d_i / d_o\right)^2\right)}\ , \tag{21}$$

and from the equation (3), the initial inner film thickness is

$$\delta_{ii} = \frac{d_i}{d_o}\delta_{oi}\ . \tag{22}$$

The initial flow rate at the inner liquid film is

$$G_{fi}^{i} = G_f\left(1 + \frac{\delta_{oi}(d_o + \delta_{oi})}{\delta_{ii}(d_i + \delta_{ii})}\right)^{-1}\ , \tag{23}$$

and at the outer liquid film

$$G_{fo}^{i} = G_f \left(1 + \frac{\delta_{ii}(d_i + \delta_{ii})}{\delta_{oi}(d_o + \delta_{oi})} \right)^{-1} . \quad (24)$$

2.4 Calculation Procedure

Calculation of initial condition: after obtaining vapor superficial velocity at the onset of annular flow by flow pattern transition criterion, quality, annular flow starting location, void fraction, and initial film thickness of inner and outer tubes are calculated subsequently.

Numerical integration: from the onset of annular flow location, the governing equations of (1) and (2) are numerically integrated along the axially nodalized channels until dryout of either the inner or outer liquid film is met or the end of the channel is reached.

Constitutive relations: first, calculating the liquid film flow rate using tube-based constitutive relations through the inner iteration of triangular relations, then mass transfer coefficient, liquid concentrations and deposition and entrainment rates of inner and outer tubes are calculated subsequently.

3. Results and Discussion

Dryout characteristics in annulus are similar to the bundle characteristics because the annulus has the cold wall or large interfacial area. The deposition and entrainment rates of the inner heated tube are relatively lower than the outer tube, and the outer film thickness is thicker than the inner liquid film in annulus. It gives the large discrepancies of CHF values on pressure between tubes and annuli, especially at a low flow rate and high quality. There are various assumption for void fraction at the onset of annular flow location. Levy assumed the void fraction of 0.80 at the onset of annular flow, but Katto reduced as 0.65 for his LFD model. Present model get ride of this the only empirical constant of LFD model by using Venkateswararo's [13] churn-to-annular flow transition model(eq. 17) that annular flow occurs at the minimum vapor velocity necessary to transport the largest entrained drop in the upward direction.

$$j_g = 3.1 \left[\frac{\sigma g(\rho_f - \rho_g)}{\rho_g^{\,2}} \right]^{1/4}$$

The vapor superficial velocity in the above equation is a function of system pressure. So, we can simply calculate the void fraction using the void-quality relationship (eq.20) with the help of the drift-flux model.

$$\alpha_{an} = \frac{x_{an}}{C_o[x_{an} + \frac{\rho_g}{\rho_f}(1 - x_{an})] + \rho_g \frac{V_{gj}}{G}}$$

The calculated void fraction at the onset of annular flow range was fell into the range of 0.32~0.85 for this model.

The experimental data of Chun et al.[15], Janssen & Kervinen[16], and Becker et al.[17] in annuli are collected, which cover the following ranges.

L/d_{he}	60	~	180 (or L/d_h, 166 ~ 445)	
Exit quality		>	0.1	
Flow rate	180	~	3300	kg / m^2 - s
Pressure	0.55	~	15	MPa

To compare the present model with the Katto model conveniently, 53 data (19 of Chun et al.; 12 of Becker et al.; 22 of Janssen & kervinen) are randomly selected in the above ranges (total 595 data exist in this range).

Figure 3 shows the predicted-to-measured CHF ratio on flow rates calculated by the tube-based Katto model (replacing the tube diameter with the heated equivalent diameter of annulus) and the present annulus LFD model. The Katto model predicts well at a high flow rate, but the prediction error becomes larger as the flow rate is lower (below 600 kg/㎡-s). The result of Figure 3-(a) shows that the Katto model could not account for the decreasing trend of CHF due to the cold wall effect in annuli at the low flow and high quality conditions as many investigators (Macbeth [7]; Doerffer et al.[8]; Park et al.[9]) observed. The present model predicts comparatively well in broad flow range as shown in Figure 3-(b). This is caused by correct modeling and assumption of the annulus characteristics, churn-to-annular flow transition, the deposition and entrainment rates of inner and outer tubes and the inner and outer film thickness. Figure 4 shows the Predition trend of present model for flow, pressure, L/Dhe, and exit quality. All the 595 data are successfully calculated in CHF prediction by the annulus LFD model with the mean of 0.99 and RMS error of 0.115 shown in Figure 5.

4. Conclusion

A liquid film dryout model for annulus geometry is suggested to calculate CHF at high vapor quality. Following conclusions can be drawn.

(a) The bundle-based flow pattern transition criterion is well fit for annular geometry, especially at a low flow rate and high quality. The calculated void fraction at the onset of annular flow range was fell into the range of 0.32~0.85.

(b) The concept of the droplet contact area fraction gives simple modeling of the deposition and entrainment rates on the liquid films of the inner and outer tubes and counts for the observed annulus characteristics of dryout phenomenon.

(c) The present model predicts well at low flow rates but tends to over-estimate at high flow rate and low quality. It may be due to the bubble generations in liquid film.

(d) Generally, the present model predicts reasonably well in the broad CHF experimental data of Chun et al., Janssen & Kervinen, and Becker et al.

Acknowledgement

This project has been carried out under the Nuclear R&D Program by MOST

NOMENCLATURE

C	concentration of liquid droplets in vapor core flow [kg m^{-3}]
C_{eq}	concentration of hydrodynamic equilibrium state [kg m^{-3}]
C_{fi}	interfacial friction factor
C_{fg}	vapor single-phase friction factor
C_o	drift coefficient
d	tube diameter [m]
d_{he}	heated equivalent diameter [m]
D	deposition rate of droplets [kg m^{-2} s^{-1}]
E	entrainment rate of droplets [kg m^{-2} s^{-1}]
g	gravitational acceleration [m s^{-2}]
G	mass velocity [kg m^{-2} s^{-1}]
G_f	total liquid film flowrate [kg m^{-2} s^{-1}]
G_{fi}	film flow of inner heated tube [kg m^{-2} s^{-1}]
G_{fo}	film flow of outer tube [kg m^{-2} s^{-1}]
G_l	liquid flow in vapor core [kg m^{-2} s^{-1}]
G^*	dimensionless mass flux
h_f	enthalpy at saturation [kJ kg^{-1}]
h_{fg}	latent heat of vaporization [kJ kg^{-1}]
h_{in}	enthalpy at inlet [kJ kg^{-1}]
j_g	superficial velocity [m s^{-1}]
k	mass transfer coefficient [m s^{-1}]
L	heated length [m]
p	pressure [MPa]
q''	heat flux [kW m^{-2}]
q^*	dimensionless heat flux
R	heated equivalent radius of annuli [m]

Λ_i Λ_i droplet contact area fraction of inner tube

Λ_o droplet contact area fraction of outer tube

Re Reynolds number

u velocity [m s^{-1}]

V_{gj} drift velocity [m s^{-1}]

x vapor quality

x_{eq} vapor quality in hydrodynamic equilibrium state

x_{ex} exit quality in CHF condition

Y_f distance perpendicular to wall [m]

z axial distance [m]

Greek letters

α void fraction

β kinematic void fraction

δ liquid film thickness [m]

δ_C critical liquid film thickness [m]

μ viscosity [kg m^{-1} s^{-1}]

ρ density [kg m^{-3}]

σ surface tension [N m^{-1}]

τ shear stress [N m^{-2}]

γ, γ' entrainment parameters

Subscripts

an onset of annular flow

f liquid

g vapor

i inner heated tube

o outer tube

w wall

Superscripts

\+ non-dimensional mark

References

[1] Whalley, P. B. (1978), "Boiling, condensation, and gas-liquid flow," Clarendon Press, Oxford, USA.

[2] Saito T, Hughes E. D. and Carbon M. W. (1978), "Multi-fluid modeling of annular two-phase flow," *Nucl. Eng. & Des*., 50, 225-271.

[3] Levy S., Healzer J.M. and Abdollanhian D. (1981) "Prediction of critical heat flux in vertical pipe flow," *Nucl. Eng. & Des*., 65, 131-140.

[4] Katto Y. (1984) "Prediction of critical heat flux for annular flow in tubes taking into account the critical liquid film thickness concept." *Int. J. Heat Mass Transfer*, Vol. 27, No. 6, 883-891.

[5] Sugawara S. (1990), "Analytical prediction of CHF by FIDAS code based on three-fluid and film-dryout model," *Nucl. Sci. & Tech*., Vol. 27, No. 1, 12-29.

[6] Hoyer, N. (1998), "Calculation of dryout and post-dryout heat transfer for tube geometry," *Int. J. Muliphase Flow*, Vol. 24, No. 2, 319-334.

[7] Macbeth R. V. (1965-66) "An appraisal of forced convection burn-out data," *Proc. Instn. Mech. Engrs*., Vol. 180 Pt 3G.

[8] Doerffer S., Groeneveld D. C., Cheng S. C. and Rudzinski K. F. (1994), "A comparison of critical heat flux in tubes and annuli," *Nucl. Eng. & Des*., 149, 167-175.

[9] Park J. W., Baek W. P. and Chang S.H. (1997), "Critical heat flux and flow pattern for water flow in annular geometry," *Nucl. Eng. & Des*., 172, 137-155.

[10] Katto Y. (1979) "Generalized correlations of critical heat flux for the forced convection boiling in vertical uniformly heated annuli." *Int. J. Heat Mass Transfer*, Vol. 22, 575-584.

[11] Hewitt, G. F. and Whalley, P. B. (1978), "The correlation of liquid entrainment fraction and entrainment rate in annular two-phase flow," AERE-R9187.

[12] Venkateswararao P., Semiat R. and Dukler A. E. (1982) "Flow pattern transition for gas-liquid flow in a vertical rod bundle," *Int. J. Muliphase Flow*, Vol. 8, No. 5, 509-524.

[13] Pushkina O. L. and Sorokin Y. L. (1969), "Breakdown of liquid film motion in vertical tubes," *Heat Transfer Sov. Res.*, Vol. 1, No 5, 56-64.

[14] Dix C. E. (1971), "Vapor void fractions for forced convection with subcooled boiling at low flow rates," *U.*

C. Berkeley.

[15] Chun S. Cha J. H. Jun H. G. Chung H. J. Chung M. K. (1997), "Critical heat flux for vertical annulus flow channel under low flow and high pressure conditions," *8TH Int. Topical Meeting on Nucl. Reactor Thermal-Hydraulics*, Kyoto, Japan, Vol. 2, 691-698.

[16] Janssen E. and Kervinen J. A. (1963), "Burnout conditions for single rod in annular geometry, water at 600 to 1400 psia," GEAP-3899*, U. S. Atomic Energy Commission*, General Electric Company.

[17] Becker K. M., Hernborg G., Bode M. and Eriksson O. (1965), "Burnout data for flow of boiling water in vertical round ducts, annuli and rod clusters," AE-177*, Aktiebolaget Atomenergi*.

[18] Kwi-Seok Ha, Jae-Jun Jeong, and Suk Ku Sim (1998), "Improvement of liquid droplet entrainment model in the COBRA-TF code," AE-177*, Korean Nuclear Society*, Vol. 30, No. 3, 181-193.

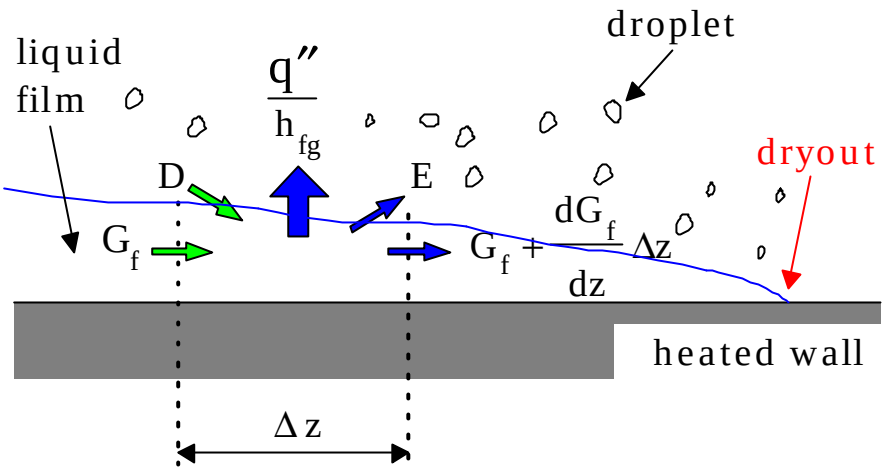

Figure 1. Control volume of liquid film dryout model

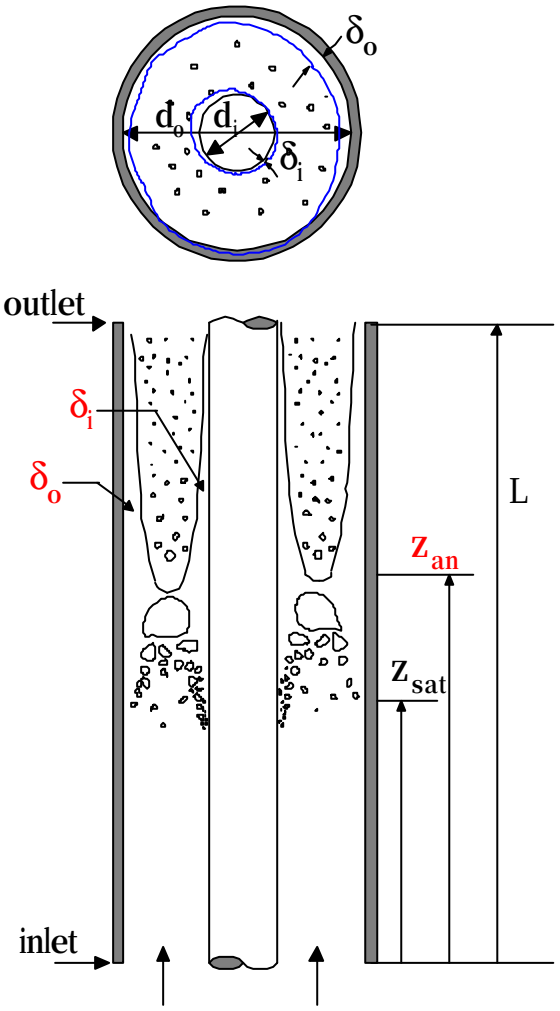

Figure 2. Cross-sectional and side view of annulus channel

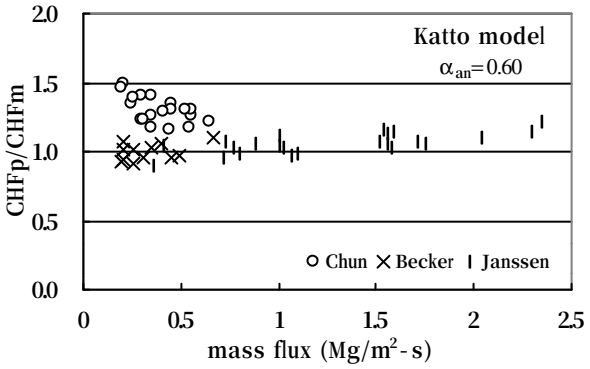

(a) Katto model

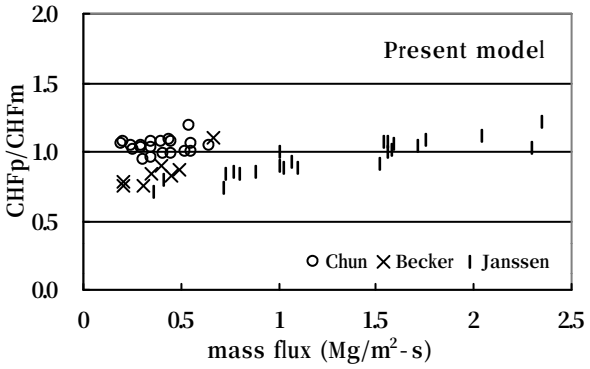

(b) Present model

Figure 3. Predicted-to-measured CHF ratio on mass flux

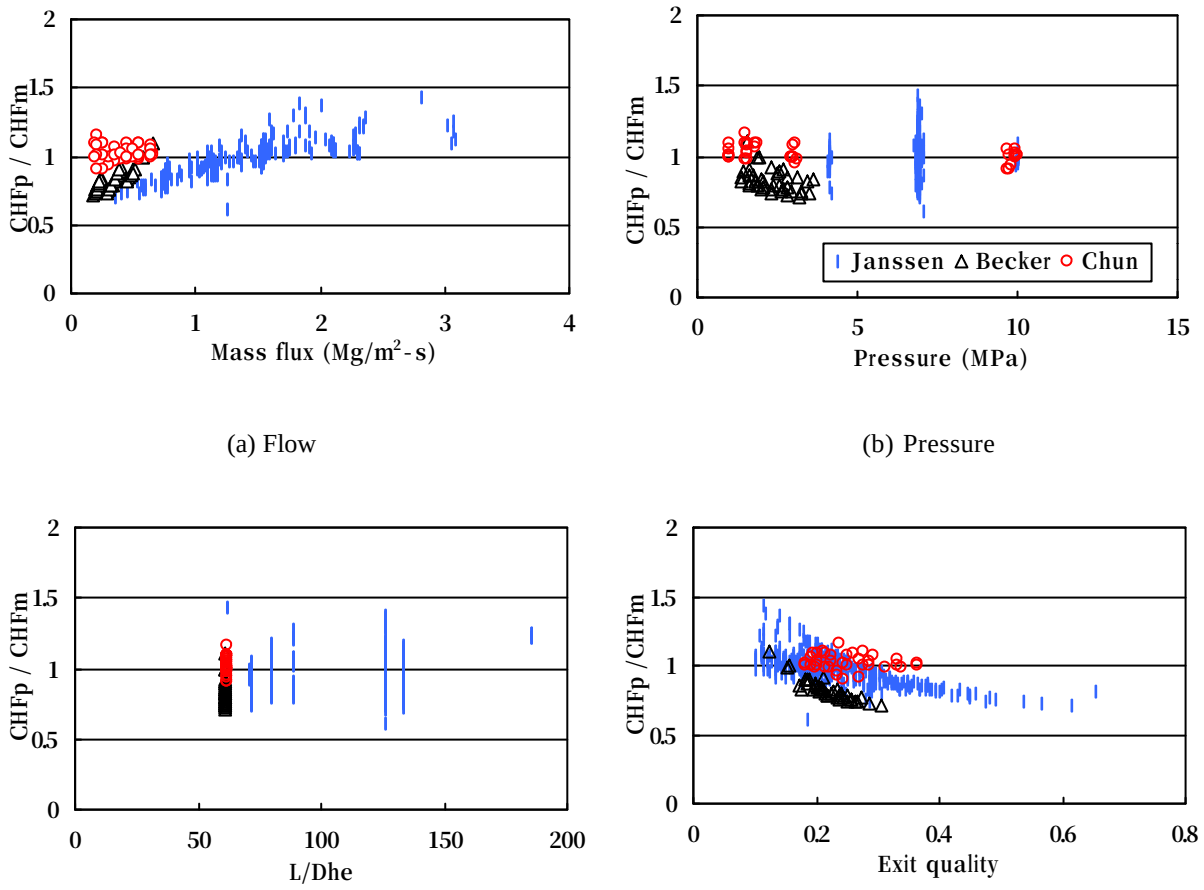

(a) Flow

(b) Pressure

(c) Length over heated equivalent diameter ratio

(d) Exit quality

Figure 4. Predition trend of present model for (a) flow, (b) pressure, (c) L/Dhe, and (d) exit quality

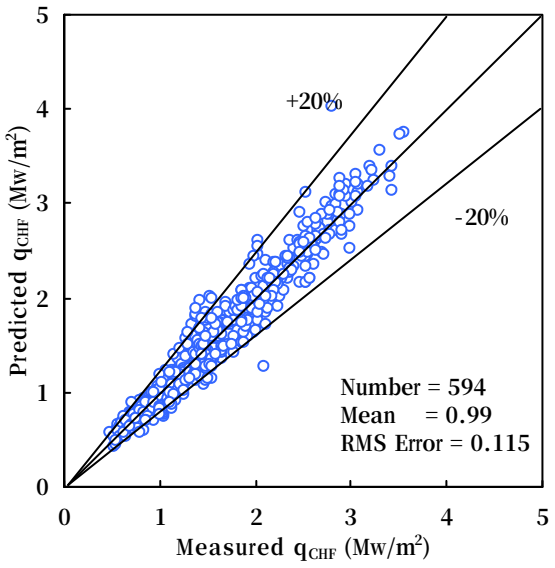

Figure 5. Predicted vs. measured critical heat flux